

# MIROS SYSTEM EVALUATION DURING STORM WIND STUDY II.

F W. Dobson

Fisheries and Oceans Canada,  
Bedford Institute of Oceanography,  
Dartmouth, Nova Scotia

E. Dunlap

ASA Consulting Ltd,  
Halifax, Nova Scotia

## 1. INTRODUCTION

The principal goal of the Storm Wind Study II (*SWS-II*) Experiment was to evaluate a variety of sensors of wind and sea state for their ability to function reliably and provide accurate and reproducible sea surface information in high sea states. The field experiment took place between 25 October 1997 and 9 April 1998 at the Grand Banks Hibernia site.

As a part of the *SWS-II* Experiment, a group of three buoys, one wave and two meteorological, was moored on 25 October 1997 at a site one nautical mile to the SW of the Hibernia Management and Development Company (*HMDC*) Platform on the Grand Banks of Newfoundland. The buoys were a standard Atmospheric Environment Service (*AES*) *Nomad* meteorological buoy, a Coastal Climate *Minimet* meteorological buoy, and a Datawell "Directional Waverider" (*DWR*) buoy.

The *DWR* buoy was operated by the Ocean Circulation Section of the Ocean Sciences Division, Canada Dept. of Fisheries and Oceans, Bedford Institute of Oceanography (*DFO/BIO*). It was deployed and recovered from the *BIO* vessel CCGS *Hudson* that was present on site during the period of 17 November to 6 December 1997.

The study location and the CCGS *Hudson's* track are indicated in Figure 1.

In addition to the standard suite of meteorological instrumentation for providing weather reports for local operations and to the World Meteorological Organization (*WMO*), an Ocean Spectra Remote

Sensing Radar (*MIROS MkII*), with a field of view that included the *SWS-II* buoys, was mounted on the Hibernia Platform.

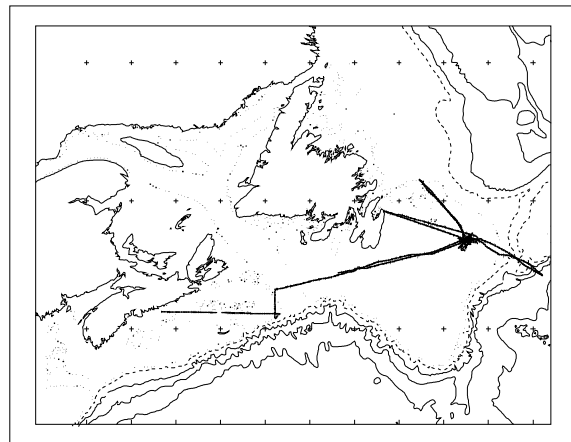


Figure 1. Map showing *SWS-II* study location and the track of the vessel CCGS *Hudson*.

The purpose of the present paper is to document the results of a comparison between the sea state parameters reported by the *MIROS* system mounted on the Hibernia Platform and the same parameters derived from the *DWR* buoy. The comparison consists of a set of time series and scatter diagrams giving the level of agreement between the two sensors in visual terms, and tables quantifying the agreement in terms of standard statistical collocation parameters.

The *MIROS* radar and *DWR* buoy data description (Section 2) is followed by short description of data analysis methods (Section 3) and presentation of the results (Section 4). The findings of this research are concluded in Section 5.

## 2. INSTRUMENTS AND DATA DESCRIPTION

### 2.1 *MIROS* radar

The C-band (5.8 GHz, 5.17 cm) *MIROS* Wave Radar is an advanced microwave sensor specifically designed for real time measurements of directional ocean wave spectra and surface current (*MIROS*, 1996). It operates at low grazing angles of about 10°. Linear wave theory is used to transform the water particle velocity spectrum, measured in the radar's pulse-Doppler mode, into the wave height spectrum. The complete unambiguous directional wave spectrum, with a frequency resolution of 0.078125 Hz and range of 0.3125 Hz, nominal directional resolution of 30° and range of 360° is formed from data collected simultaneously from two radar footprints less than one half wavelength apart.

Based on the two-dimensional spectrum the point spectrum, as well as the spectral and integrated scalar wave parameters are calculated. The *MIROS* radar measures wave height, period and direction with an accuracy of ±5% (in the range 0.2 to 20 m), ±5% (in the range 3 to 30 s), and ±7° (in the range 0 to 360°). The data from the *MIROS* system consisted of a tabular file containing a set of 28 "standard" wave and surface current parameters (*MIROS*, 1996).

A subset of the integrated wave parameters was used in the comparison with the *DWR* buoy measurements. *MIROS SWS-II* data were available for the period starting on 29 December 1997 and ending on 10 June 1998.

### 2.2 *DWR* buoy

The *DWR* buoy (Datawell S/N 30070) is a spherical buoy, 0.9 m diameter that contains heave/pitch/roll sensors: *i.e.* a three axis fluxgate compass, one vertical and two horizontal fixed accelerometers, and a microprocessor. From the horizontal (corrected to north and west) and vertical acceleration measurements, the corresponding displacements are obtained using digital integration. The buoy sampling frequency is 1.28 Hz (1536 samples in a 20-min data acquisition period) and its "Nyquist" frequency (max frequency resolved) is 0.64 Hz. The buoy processor computes the variance spectrum of the vertical motion with a frequency resolution of 0.005 Hz for frequencies less than 0.1 Hz and 0.01 Hz up to 0.58 Hz. It also computes parameters of the directional distribution, *i.e.* the auto-, co- and quadrature variance of the vertical, North and West motion are calculated for each

frequency band (Datawell, 1992). The pre-experiment calibration indicates that the buoy heave measurement is 0.3% low at wave periods up to 12.5 sec and 4.5% low at 20 sec period; the direction accuracy is within 1°; the spreading error is approximately 3°, and the overall ability to compute the wave dispersion relation (a measure of the combined heave and wave frequency determination errors) is about 4% at 6 sec periods, 10% at 12.5 sec periods, and 25% at 20 sec periods (Datawell, 1996).

The buoy provided data once per hour, covering the full time period from 25 October 1997 to 9 April 1998. The non-directional spectral parameters were computed from two 13 minute time series starting 12 and 41 minutes past the hour. This data set is complete (with the exception of few hours) for the whole period of the experiment. The parameters of the directional distribution were derived at run time from 20 min time series starting at 10 min before the hour. This time series has a one month gap from 30 November to 29 December 1997.

An estimate of the directional wave spectrum has been obtainable from time series of heave, pitch and roll since Lonquet-Higgins, Cartwright and Smith (1963) introduced a direct Fourier transform method to extract directional spectrum estimate from buoy data. Many spectral estimators are now available. The most commonly used estimators include the Maximum Likelihood Method (*MLM*: Capon, 1969; Isobe *et al.*, 1984) and its extensions (Oltman-Shay and Guza, 1984; Mardsen and Juszko, 1987; Brissette and Tsanis, 1994), as well as the Maximum Entropy Method, (*MEM*: Lygre and Krogstad, 1986).

An estimate of a full *MLM* directional wave spectrum (with a frequency resolution of 0.005 Hz and a range from 0.025 Hz to 0.58 Hz and directional a resolution of 5° and range from 21.8° to 376.8°) was obtained from the *DWR* parameters of the directional distribution. The *MLM* method was used, despite its tendency to over-predict the angular spreading, because it is relatively insensitive to extraneous factors such as presence of noise and the wavenumber dependence (Brissette and Tsanis, 1992). The *MLM* method provides a relatively easy to implement, efficient and robust estimator. An example of the full *DWR-MLM* wave spectrum (*i.e.* derived from the *MLM* spectral analysis of the buoy data) is shown in Figure 2 while the corresponding power and mean direction spectra are shown in Figure 3.

MLM spectrum: 21 November 1997 15:34 GMT.

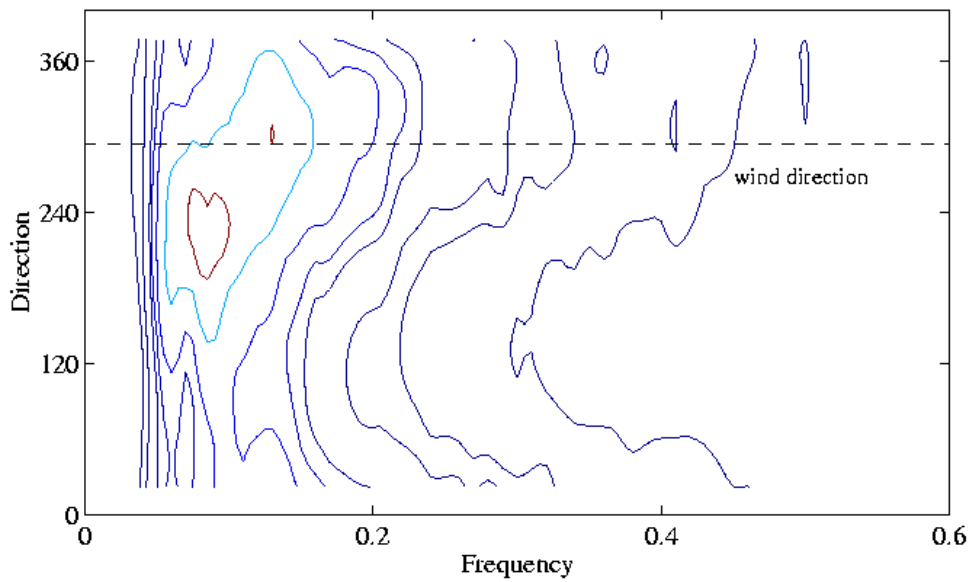
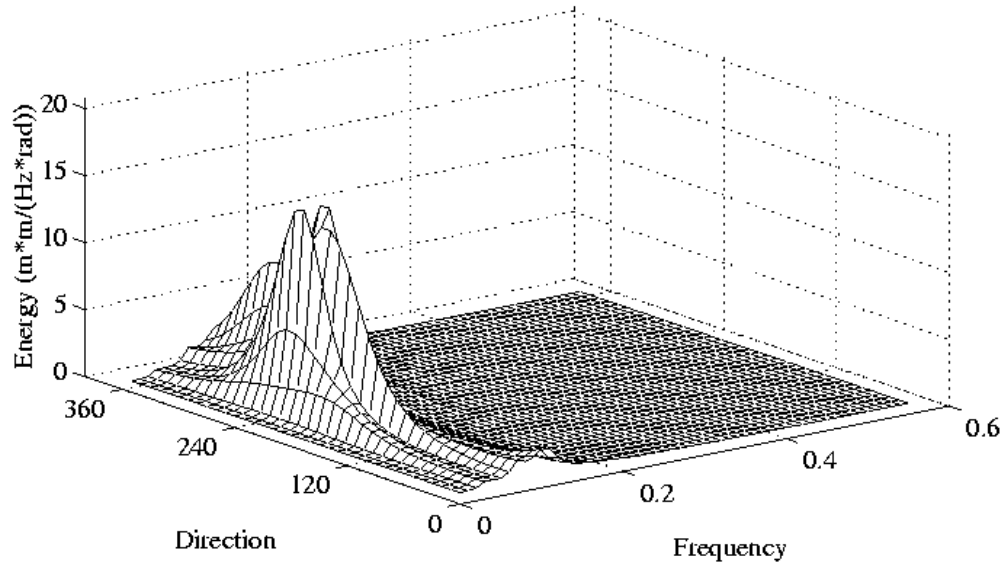


Figure 2. Sample full *MLM-DWR* directional wave spectrum. Upper panel is a 3-dimensional mesh representation, lower is a contoured representation. Contours are spaced logarithmically to show high-frequency behavior.

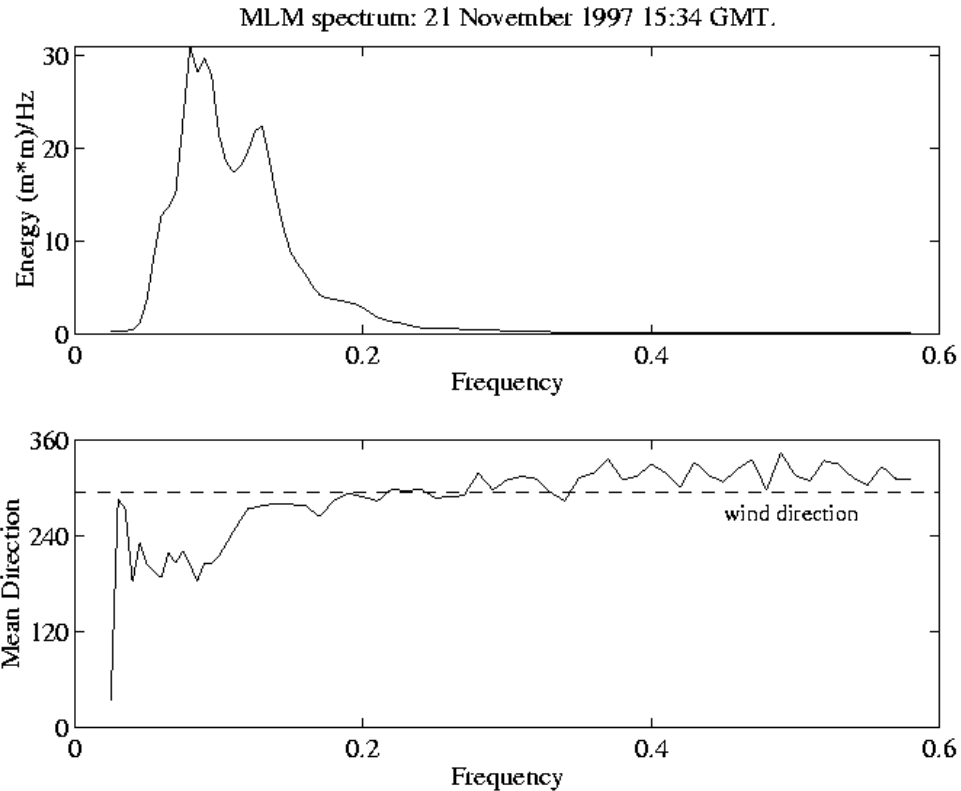


Figure 3. Sample *MLM-DWR* wave power (upper) and mean direction (lower) spectra.

The significant wave height, peak period, peak and mean directions of the data sample shown in Figures 2 and 3 are:  $H_{m0}=6$  m,  $T_{p1}=12.5$  s,  $D_{m1}=219.5^\circ$ , and  $D_{p1}=221.8^\circ$ , respectively (see Appendix A for the definition of wave spectral parameters). Sample wind speed is equal to 25.43 m/s and wind direction is  $293.7^\circ$ .

### 3. DATA PROCESSING AND ANALYSIS

During processing it became clear that both the *MIROS* and *DWR* data sets contained "outliers" or "bad" values. In the course of the analysis traps were inserted and software written to correct, remove or interpolate over such deficiencies (Dunlap, 1999).

Inspection of the *MIROS* data set showed that during the period between 14 March and 9 May 1998, the radar produced erroneous wave period (but apparently correct wave height) information. This data set was filtered out prior to comparison with *DWR* data. After the preliminary quality control, the filtered *MIROS* spectral parameters and the corresponding parameters derived from the *DWR-MLM* wave spectra were

interpolated to the center time of the buoy averaging interval once per hour.

The collocated observations from the two systems (*MIROS* and *DWR*) were then used to produce scatter plots and the overall statistics of the variability and co-variability of the two sea state sensing systems.

## 4. DATA ANALYSIS RESULTS

### 4.1 Time series

The time series of selected spectral parameters, i.e. the significant wave height ( $H_{1/3}$  or  $H_{m0}$ ), significant period ( $T_{1/3}$  or  $T_{p1}$ ) and maximum period ( $T_{max}$ ) measured by the *MIROS* and *DWR* systems are shown in figures 4, 5, and 6, respectively (see Appendix A for the corresponding definitions).

The nature of the *MIROS* wave period data changes significantly, showing anomalous values in the time period between 14 March and 9 May 1998. It appears to be "restored" to its initial state after that period. Since the *DWR* time series begin on 25 October 1997 and end on 9 April 1998 the comparison between *MIROS* and *DWR* data was confined to the time period 29 December 1997 to 14 March 1998.

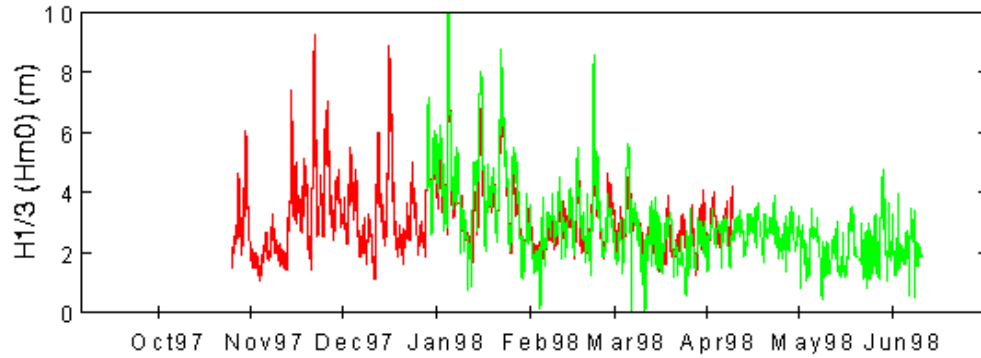


Figure 4. Time series of *DWR H1/3* (red/black) and *MIROS Hm0* (green/gray). Minimum *Hm0* in *MIROS* data is equal to 1 cm.

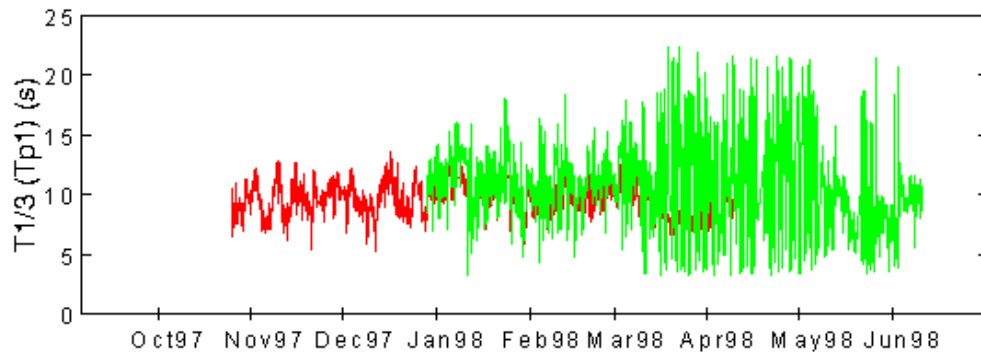


Figure 5. Time series of *DWR T1/3* (red/black) and *MIROS Tp1* (green/gray).

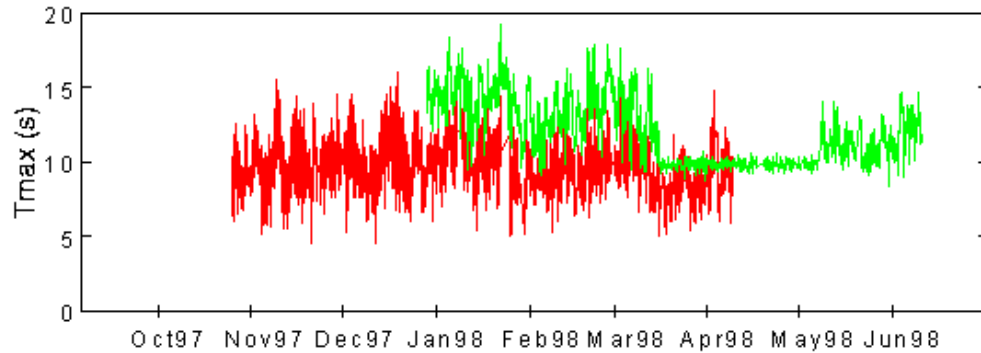


Figure 6. Time series of *Tmax* for *DWR* (red/black) and *MIROS* (green/gray).

#### 4.2. Scatter plots

The following scatter plots (Figures 7 through 9) are the comparison of the collocated and filtered out *MIROS* and *DWR-MLM* main wave spectral parameters. The scatter plots summarize the comparison in terms of correlations for the integrated wave parameters. They are Joint Probability

distributions of the *MIROS* and *DWR MLM* data sets. The scatter plots for the five remaining spectral parameters investigated in this study are summarized in Appendix B.

The collocation statistics are based on data samples that have been subjected to quality control and cover only the time period from 31 December 1997 to 9 April

1998. The corresponding statistical analysis for all eight spectral parameters investigated in this study is given in the Section 4.3.

For each parameter the two versions of each plot, *i.e.* contoured (left panel) and scatter (right panel), provide the means to see both the distribution that forms the correlation statistics and the groupings of the individual pairs that make up the distribution.

The large range of wave heights and periods typifies the stormy conditions encountered in the North Atlantic Ocean during the winter months. In general terms, the height distributions are the better-formed and demonstrate the tight link between the observations made by the two instruments. The period distributions

are more scattered and cover a narrower range of values; their correlations are not as strong as are the height correlations. The least well-defined are the distributions of wave direction. This represents, to some extent, the cyclic nature of the direction parameters (they "wrap" at  $0^\circ/360^\circ$ ) but also demonstrates the inherent difficulty experienced with both sensors in defining wave direction.

The plots indicate that the *MIROS* system is well-calibrated for both height and period. It overestimates the wave height slightly at large heights and underestimates at low heights and is in statistical agreement with the *DWR* for wave period. It appears to be biased about  $20^\circ$  low in direction relative to the *DWR* (corrected from magnetic to true direction).

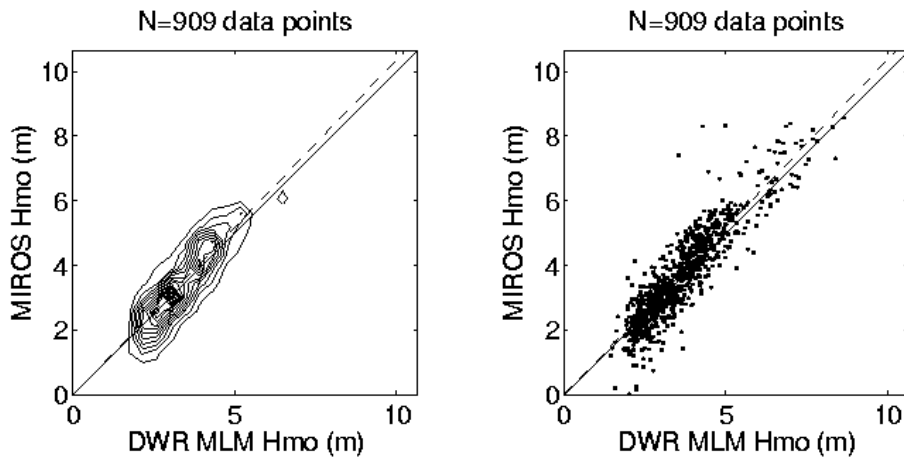


Figure 7. Significant wave height comparison.

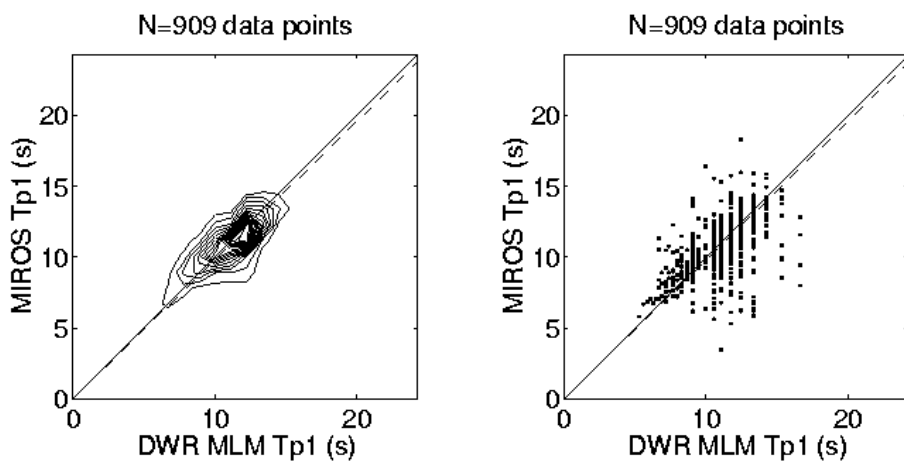


Figure 8. Comparison of periods at primary spectral peak.

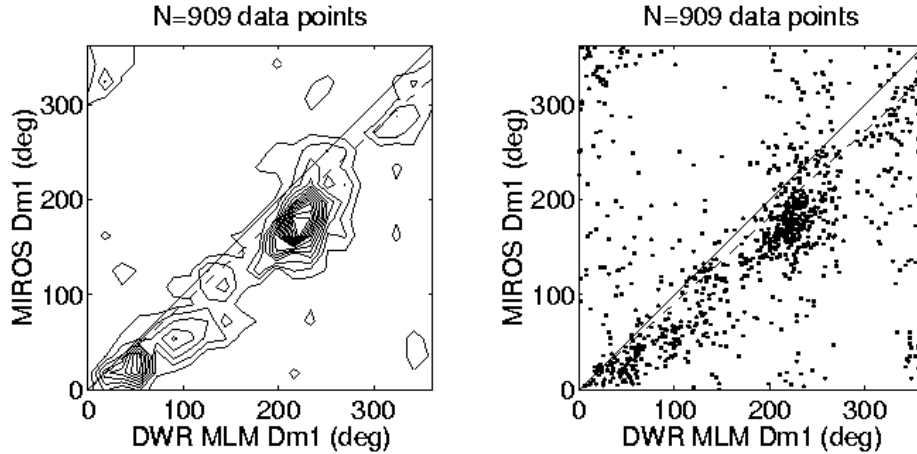


Figure 9. Comparison of mean wave direction.

#### 4.3 Statistical comparisons

The statistical comparisons provide a quantified version of the visual evidence in the time series and scatter plots. The comparison of a full set of spectral parameters used in this work (as defined in the Appendix A) is given in Tables 1 and 2.

These tables give a standard list of statistical measures of the comparisons for the *MIROS* data vs the *DWR-MLM* data for a set of eight wave parameters for the "filtered" data set. Here "filtered" implies not only that all outliers and "bad" data values have been removed but also that the comparison has been stopped at 14 March 1998, when the wave periods from the *MIROS* system indicate distinct problems.

Table 1. Means and standard deviations for collocation of filtered *MIROS* vs *MLM* centered at *DWR* times. Number of samples is 909.

<i>Parameter</i>	<i>Units</i>	<i>mean</i> <i>(DWR)</i>	<i>mean</i> <i>(MIROS)</i>	<i>bias</i> <i>(MIROS-DWR)</i>	<i>std(X)</i> <i>(DWR)</i>	<i>std(X)</i> <i>(MIROS)</i>
<i>Hm0</i>	m	3.55	3.61	0.06	1.17	1.42
<i>Hmax</i>	m	6.40	5.78	-0.61	2.10	2.24
<i>Tp1</i>	Sec	11.3	11.0	-0.26	1.78	1.83
<i>Tz</i>	Sec	7.32	7.46	0.14	0.84	0.84
<i>Tav</i>	Sec	8.72	8.12	-0.60	0.95	0.91
<i>SDp1</i>	m <sup>2</sup> /Hz	18.7	19.1	0.31	17.6	19.4
<i>Dp1</i>	Degrees	173	155	-18	97	93
<i>Dm1</i>	Degrees	180	160	-20	97	93

Table 2. Slope, correlation and scatter index for collocation of filtered *MIROS* vs *MLM* centered at *DWR* times. Number of data samples is 909.

<i>Parameter</i>	<i>slope</i>	<i>Corr<sub>0</sub>(%)</i>	<i>Corr<sub>m</sub>(%)</i>	<i>SI<sub>0</sub>(%)</i>	<i>SI<sub>m</sub>(%)</i>
<i>Hm0</i>	1.04	98.7	89.9	17.6	22.2
<i>Hmax</i>	0.92	98.7	89.5	16.5	17.8
<i>Tp1</i>	0.98	98.9	58.3	14.8	11.6
<i>Tz</i>	1.02	99.6	65.8	9.4	11.4
<i>Tav</i>	0.93	99.6	69.2	8.7	11.6
<i>SDp1</i>	1.06	91.0	81.8	59.8	17.8
<i>Dp1</i>	0.91	84.9	40.2	63	6
<i>Dm1</i>	0.91	86.0	41.4	60	6

The **MIROS** system underestimates significant wave height **Hm0** relative to the **DWR** at low wave heights and (excepting some notable outlying underestimates) slightly overestimates **Hm0** overall - by 4%, with a bias of 0.06 m. The mean of the **MIROS Hm0** distribution is 2% greater than the **DWR**, and the **MIROS** wave variance exceeds the **DWR Hm0** variance significantly. The much larger **MIROS Hm0** variance is evident in the time series plots, and as a group of points on the scatter plot that may be treatable as outliers using advanced statistical techniques. The 99% correlation indicates it is not a severe problem, and in general the **MIROS** is a first-class wave height sensor over the full range of conditions expected at the Hibernia site.

The wave period parameters (**Tp1**, **Tz**, **Tav**) observed cover the 5-15 sec range, and the comparison statistics indicate excellent agreement, with correlations of 99%, slope of 0.93 - 1.02 and biases of -0.6 to 0.1 sec (**MIROS** low). The overall means agree well, and so do the **MIROS** variances, indicating the **MIROS** slightly underestimates the period in the mean and slightly overestimates the period variance; this is borne out in the time series and scatter plots.

Although the primary wave spectral density **SDp1** varied over the range 0-150 m<sup>2</sup>/Hz, most of the points are clustered in the range < 50 m<sup>2</sup>/Hz. As with **Hm0**, there were **MIROS** "outliers" at high values that bias the **SDp1** variance high while the mean agrees well with the **DWR**. The 91% correlation has a slope of 1.06 and a bias of essentially zero. The direction comparisons are less well-defined; the correlations are 85% with slopes of 0.91 (**MIROS** underestimates direction by 9%), biases of 18°-20° (**MIROS** low) and high scatter indices. Note that both instruments have been corrected to true heading (the compass variation in the Hibernia area is 21° West).

Experience with the **DWR** direction determination capabilities indicate that at short wave periods it indicates the wind direction within 5° with an rms scatter of 10° about the mean of the highest 10 spectral estimates. The radar system should, by the nature of the direction determination process in the instrument, do at least as well as the **DWR**. The suspicion is that the direction of the waves at the primary peak (often due to swell at the Hibernia site) is highly variable with frequency and the observed scatter in the comparisons is at least partly due to the two instruments choosing slightly differing frequencies/periods for the "primary peak".

## 5. DISCUSSION AND CONCLUSIONS

The quantitative evaluation of the **MIROS** system using the **DWR** as a standard is limited due to the presence of errors. Some types of error are listed below.

First is the expected error associated with the instruments themselves. In the case of **MIROS** this will include the radiometric calibration of the radar itself, the antenna pattern corrections and their accuracy, the velocity accuracy of the Doppler system, and the effects of side lobe reflections/refraction from objects near its mounting location on the Platform. In the case of the **DWR**, this will include the accuracy of the individual accelerometers used to measure the pitch, roll and heave of the buoy, and the accuracy of corrections for the response function of the buoy itself. The second source of error is "algorithm error". Included in this category will be the accuracy of the algorithms used to convert the signals received by the radar into wave parameters, and the accuracy of the algorithms used in converting the **DWR** Fourier coefficients into "equivalent" wave parameters. The third (and by no means the least significant) source of error is "sampling error". This accounts for the fact that ocean waves are highly variable in both space and time. It is never possible (and certainly not in this comparison) for two sensors to view exactly the same wave field at the same time. In this case, the **MIROS** system took a spatial average of the wave field over the radar footprint area and a temporal average of that field over a time period of 20 min. The **DWR**, although it was contained within the field of view of the radar, took a 20 min time average of the waves that passed its location.

Lastly, although there is no guarantee that the wave parameters vary smoothly in time, this assumption is built in to this comparison by the performance of the linear interpolation used to collocate the observations in time. It is expected from the above that agreement will be confined to the "generalities" of the wave field (that is, the overall statistics as represented by the wave parameters for which this comparison is made) rather than the particulars of each individual pair of observations being compared.

There is a single important deficiency in the **HMDC MIROS** installation uncovered by this study. If the data set is a reflection of what is gathered in the operational setting, the period between 14 March and 9 May 1998, when the radar produced erroneous wave period information (but apparently correct wave height), is a sign that some form of continuous quality control is required in real time.



In general terms, setting aside the section of "bad" **MIROS** wave period estimates, based on the statistical measures used in this analysis, the agreement of the **MIROS** and **DWR** wave measurements is excellent. With one exception (the 15° bias in indicated wave direction of the **MIROS** system) the radar has proven itself in this study to be the equivalent of a well-calibrated directional wave buoy in determining the sea state parameters important to the regulators for reasons of safety and to the engineers for design purposes. Since the study includes a range of 0-10 meters in significant wave height (and 18 meters in **Hmax**) and 5-18 sec in wave period, the **MIROS** system appears to be capable of dealing with the most severe storms likely to occur on the Grand Banks in winter.

#### ACKNOWLEDGMENTS

This work has been carried out as part of the Storm Wind Study II, (**SWS-II**), under the overall leadership of Mr. Val Swail of the Atmospheric Environment Service (**AES**), Environment Canada and funded by the Panel for Energy Research and Development (**PERD**). The data from the **MIROS** system were kindly supplied by K. G. Dyer, Environment, Safety and Quality Advisor to **HMDC**. The **HMDC** Platform staff assisted in a number of ways, including the provision of space on the Platform for telemetry receivers and recording systems for the buoys, and the archiving of the **DWR** telemetry data. We acknowledge the professional assistance of the Captain and crew of CCGS **Hudson** in deploying and recovering the **DWR** buoy.

#### APPENDIX A. DEFINITIONS OF WAVE PARAMETERS AND STATISTICAL MEASURES.

The following spectral parameters were used:

Full directional spectrum:	$P(f, \theta)$
Point spectrum:	$S(f) = \sum P(f, \theta) d\theta$
Spectral moments:	$m_n = \int f^n S(f) df$
Surface elevation variance:	$VARn = m_0$
Significant wave height:	$HM0 = H_s = H_{1/3} = 4\sqrt{m_0}$
Primary wave peak period:	$Tp1 = \frac{1}{f_p}$ where

	$S(f_p) = \max(S(f))$
Primary wave spectral density	$SDp1 = S(f_p)$
Primary wave mean direction:	$Dm1 = ATAN\left(\frac{\sum \sin(\theta) \cdot P(f_p, \theta) d\theta}{\sum \cos(\theta) \cdot P(f_p, \theta) d\theta}\right)$
Primary wave peak direction:	$P(f_p, Dp1) = \max(P(f_p, \theta))$
Mean zero up-crossing period:	$Tz \approx Tm02 = \sqrt{\frac{m_0}{m_2}}$
Mean period:	$T_{av} = \sqrt{\frac{m_{-1}}{m_1}}$

The statistics shown in tables 1 and 2 were computed as follows:

Sample mean:	$\langle X \rangle = \frac{1}{N} \sum_{i=1}^N X_i$
Sample standard deviation	$std(X) = \sqrt{\text{var}(X)} = \sqrt{\frac{1}{N} \sum_{i=1}^N X_i^2 - \langle X \rangle^2}$
Bias:	$bias = \langle Y \rangle - \langle X \rangle$
Slope of linear regression line:	$slope = \frac{\sqrt{\langle Y^2 \rangle}}{\sqrt{\langle X^2 \rangle}}$
Correlation coefficient about zero:	$Corr_0 = \frac{\langle X \cdot Y \rangle}{\sqrt{\langle X^2 \rangle \langle Y^2 \rangle}}$
Correlation coefficient about the mean:	$Corr_m = \frac{Co \text{ var}(X, Y)}{\sqrt{\text{var}(X) \text{ var}(Y)}}$
Scatter index about the mean:	$SI_m = \frac{\sqrt{\text{var}_D(X, Y)}}{\sqrt{\langle X \rangle \langle Y \rangle}}$
Scatter index about zero:	$SI_0 = \frac{\sqrt{rms_D(X, Y)}}{\sqrt{\langle X \rangle \langle Y \rangle}}$
Covariance:	$Co \text{ var}(X, Y) = \frac{1}{N} \sum_{i=1}^N (Y_i - \langle Y \rangle)(X_i - \langle X \rangle)$
Variance of a difference:	$\text{var}_D = \frac{1}{N} \sum_{i=1}^N (Y_i - X_i - bias)^2$
Root mean square of a difference:	$rms_D = \frac{1}{N} \sum_{i=1}^N (Y_i - X_i)^2$

APPENDIX B. SUBSET OF SCATTER PLOTS  
USED IN COLLOCATION ANALYSIS

The scatter diagrams for the five wave spectral parameters used in the collocation statistics (Tables 1 and 2) but not shown in Section 4.2 are summarized in Figures B1 through B5.

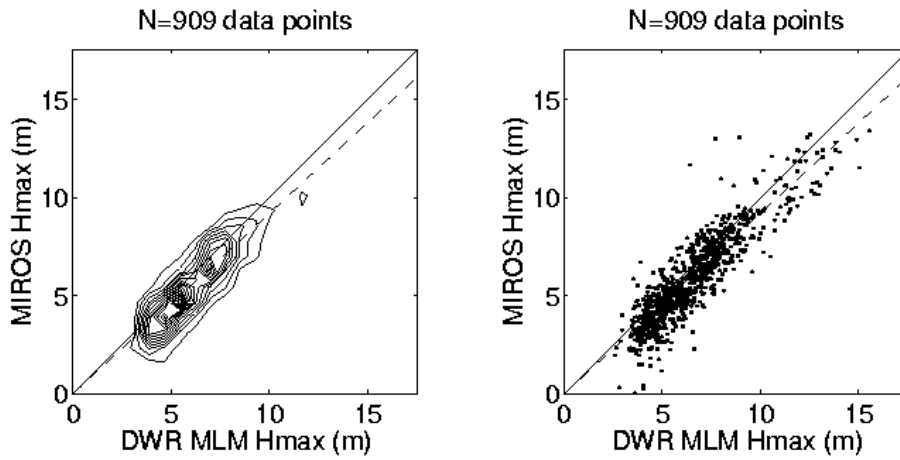


Figure B1. Maximum wave height comparison.

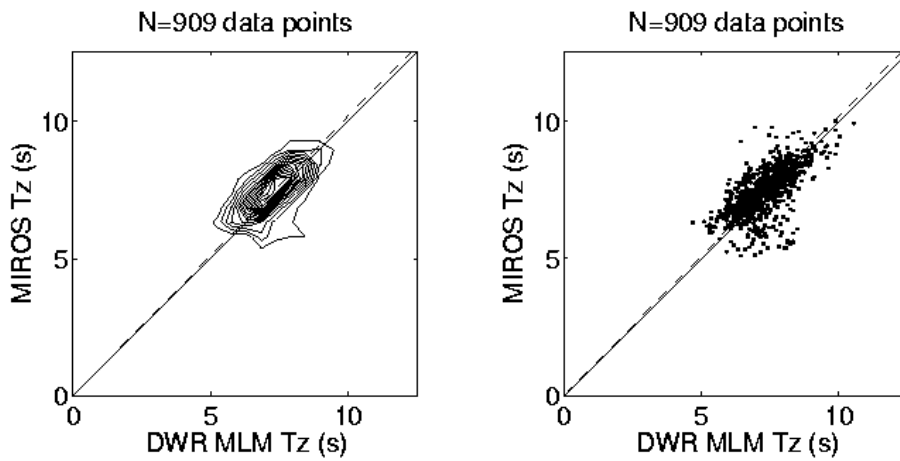


Figure B2. Comparison of mean zero-crossing period.

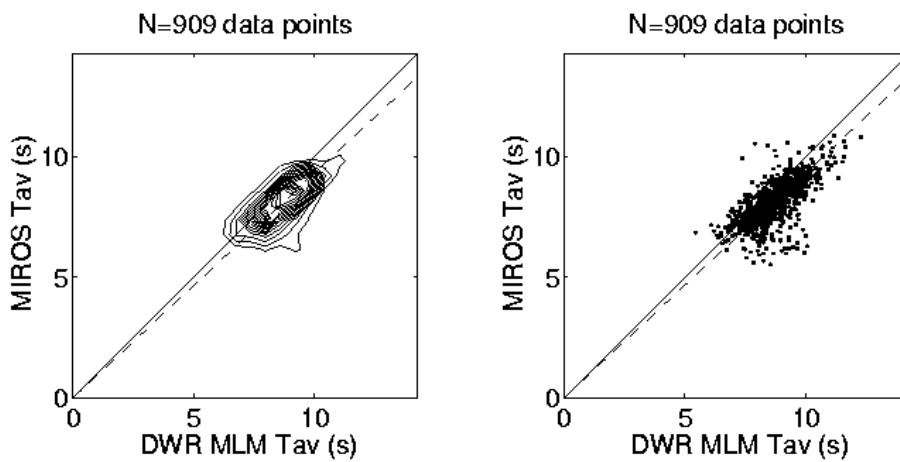


Figure B3. Comparison of mean period.

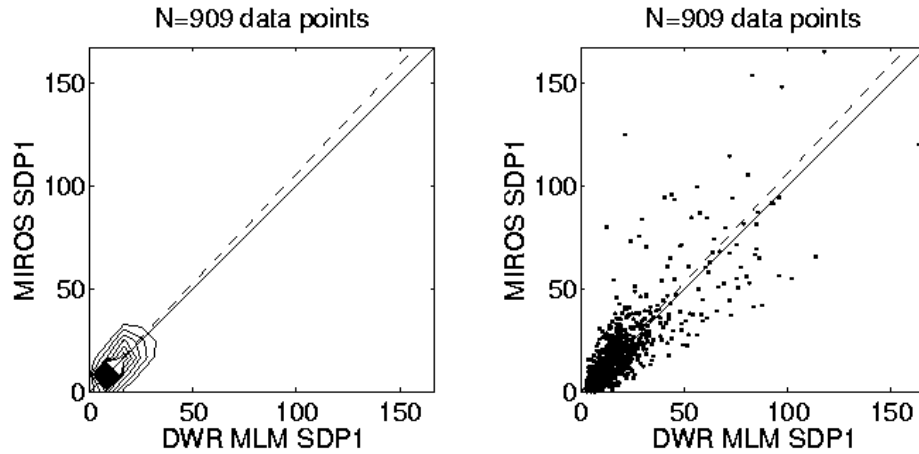


Figure B4. Comparison of spectral density at primary peak.

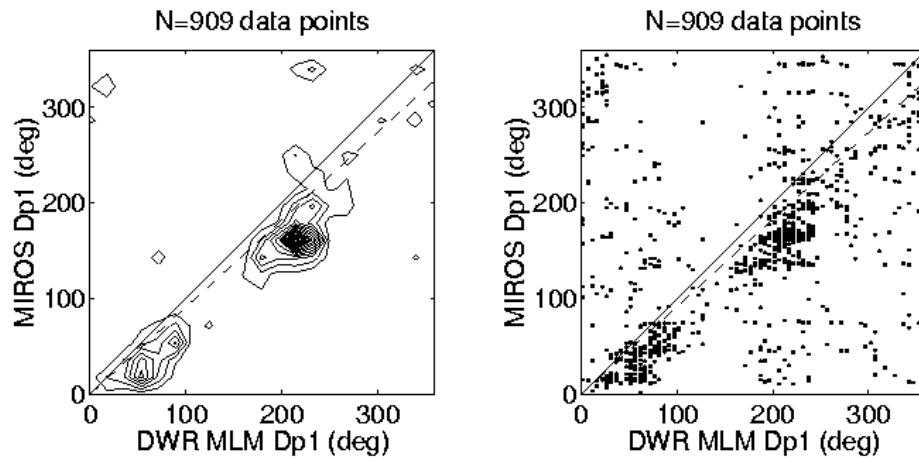


Figure B5. Comparison of wave direction at primary spectral peak.

## REFERENCES

- Brissette, F. P., and Tsanis, I.K., 1992: Maximum Likelihood Method techniques for the directional analysis of heave-pitch-roll data. *Proc. 3<sup>rd</sup> International Workshop on Wave Hindcasting and Forecasting*, Montreal, May 19-22, 1992. EC-AES, Downsview, Ontario, 1-11.
- Brissette, F. P., and Tsanis, I.K., 1994: Estimation of directional wave spectra for pitch-roll buoy data. *Journal of Waterway Port Coastal and Ocean Engineering*, 120, 93-118.
- Capon, J., 1969: High-resolution frequency-wavenumber spectrum analysis. *Proc. IEEE*, 57, 1408-1418.
- Datawell, 1992: Warec – PC Software. *Datawell Laboratory for Instrumentation*. Haarlem, Netherlands.
- Datawell, 1996: Operational Manual - Buoy Specifications. *Datawell Laboratory for Instrumentation*, Haarlem, Netherlands.
- Dunlap, E., 1999a. Air-sea interaction data analysis for the Storm Wind Study II Experiment. *Technical Report ASA 9810*, ASA Consulting Ltd., Halifax, Canada.
- Isobe, M., K. Kondo, K. Horikawa, 1984: Extension of MLM for estimating directional wave spectrum. *Symposium on Description and Modelling of Directional Seas*. June 18-20, Technical University, Denmark.
- Longuet-Higgins, M. S., D. E. Cartwright and N. D. Smith, 1963: Observations of the directional spectrum of the sea waves using the motions of the floating buoy. *Ocean Wave Spectra*, Prentice-Hall, 111-136.

Lygre, A., and Krogstad, H. E., 1986: Maximum entropy estimation of the directional distribution in ocean wave spectra. *J. Phys. Oceanogr.*, 16, 2052-2060.

Mardsen, R.F. and Juszko, B. A, 1987: An eigenvector method for calculation of directional wave spectra from heave, pitch and roll buoy data. *J. Phys. Oceanogr.*, 17, 2157-2167.

MIROS, 1993: MIROS wave radar MkII. DF-005/WR Data Format Description. *Hibernia Development Project*, St. John's, Newfoundland.

Oltman-Shay, J., and Guza, R. T., 1984: A data adaptive ocean wave directional spectrum estimator for pitch/roll type measurements. *J. Phys. Oceanogr.*, 14, 1800-1810.